Supporting Information

for "A Visual Sensor for Sterilization of Polymer Fixtures Using Embedded Mesoporous Silicon Photonic Crystals"

ACS Sensors
Manuscript ID: se-2017-00764d

*Tushar Kumeria[1,2‡], Joanna Wang[3‡], Nicole Chan[1], Todd Harris[4], and Michael J. Sailor[1]**
[1] Department of Chemistry and Biochemistry, University of California, San Diego, 9500 Gilman Drive, La Jolla, CA 92093, United States

[2] School of Pharmacy, University of Queensland, 20 Cornwall Street, Woolloongabba, QLD-4102, Australia

[3] Materials Science and Engineering Program, University of California-San Diego, 9500 Gilman Drive, La Jolla, CA 92093, United States

[4] Sienna Biopharmaceuticals Inc. 30699 Russell Ranch Road, Suite 140, Westlake Village, CA 91362, United States

Corresponding Author:
*E-mail: msailor@ucsd.edu

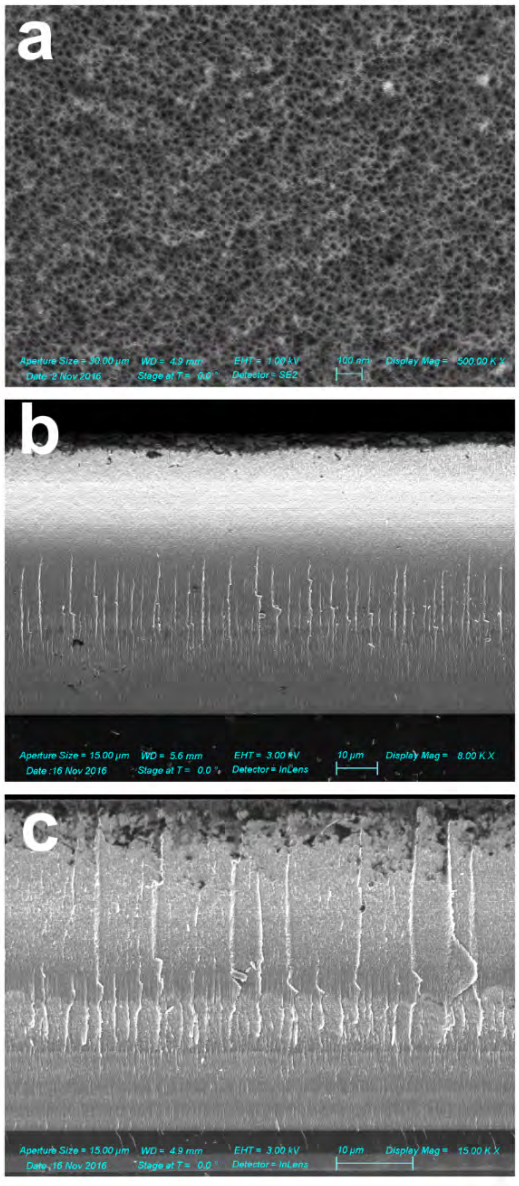

Figure S1. Scanning electron microscope (SEM) Images of Porous Silicon Photonic Crystal Templates. **(a)** Plan-view image representative of all the pSi templates used in this study, revealing the pore morphology. The mean pore diameter of the porous layer was 19 ± 7 nm, determined from the plan-view image using the ImageJ image processing software package (NIH). **(b)** Cross-sectional SEM image of the pSi template used to prepare the all-polymer photonic sensors (thickness 43.0 ± 0.2 µm). **(c)** Cross-sectional SEM image of the pSi template used to prepare the composite photonic sensor (thickness 67.3 ± 0.3 µm). These images were acquired in secondary electron imaging mode, using a Zeiss Sigma 500 SEM operating at an accelerating voltage of 1 kV (a) or 3 kV (b and c). The all-polymer and composite sensors that resulted from these templates displayed thicknesses of 37 ± 2 µm and 61 ± 4 µm, respectively (images not shown).

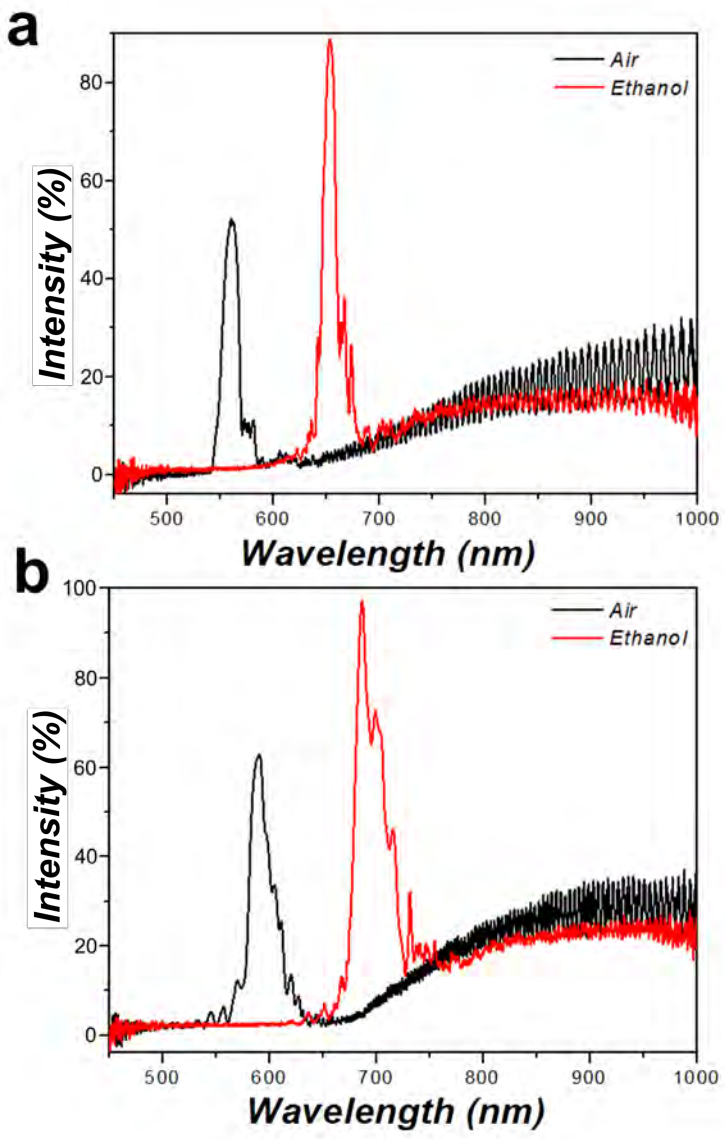

Figure S2. Optical reflection spectra of pSi templates used to prepare (a) the all-polymer sensor and (b) the pSi-polymer composite sensor. Both panels present reflectance spectra measured on the samples in air (black trace) and immersed in ethanol (red trace). These spectra, acquired before and after wetting of the porous nanostructure with ethanol, are used to determine the thickness and porosity of the pSi template. The red shift in the spectrum derives from the increase in average refractive index of the film when the air (n = 1.000) in the porous nanostructure is replaced with ethanol (n = 1.361). The degree of spectral shift is related to the average refractive index of the pSi skeleton and the average porosity of the film.[1] To obtain open porosity and thickness, measured values of effective optical thickness were fit to a two-component Bruggeman effective medium approximation. For the template used to prepare the all-polymer sensor, the porosity and thickness of the pSi template were 61 ± 1 % and 38 ± 2 µm, respectively. For the template used to prepare the composite sensor, the porosity was 60 ± 2 % and the thickness was 61 ± 4 µm. These spectra were obtained on the as-etched pSi templates, prior to thermal oxidation.

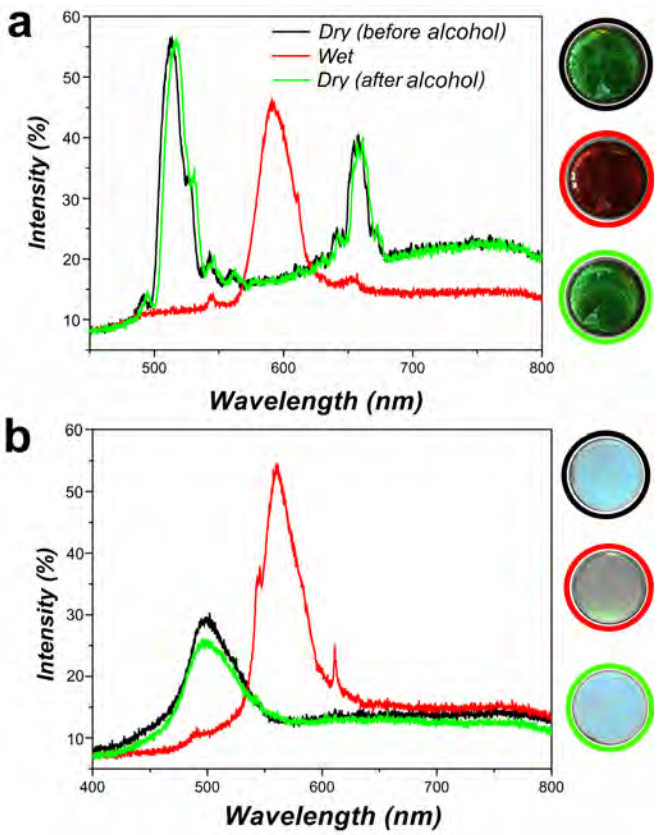

Figure S3. Optical reflection spectra and photographs of pSi-polycarbonate composite (a) and all-polymer (b) samples used to characterize the templating and alcohol sensing properties. (a) Optical reflection spectra of the dry pSi-polymer composite (black trace), the pSi-polymer composite wetted with 70 % isopropyl alcohol (red trace), and the pSi-polymer composite after the alcohol solution has dried for ~ 2 min in air (green trace). The pSi-polymer composite was prepared by partial infiltration (thermal casting) of a polycarbonate sheet as described in the text. Because the pSi film is only partially infiltrated with polycarbonate, the sample displays two stop bands. The stop band at 520 nm corresponds to the empty portion of the pSi layer (not filled with polycarbonate) and the band at 660 nm corresponds to the portion of the pSi layer that is filled with polycarbonate. Upon wetting with alcohol, the stop band at 520 nm (the empty portion of the pSi film) shifts to 600 nm and the stop band at 660 nm displays a negligible shift. The 660 nm band appears weak in the wetted sample relative to the 600 nm band because the spectra are not corrected for the instrument response function or the tungsten halogen lamp intensity distribution. The tungsten halogen light source has relatively low intensity in the blue-green region of the spectrum. Photographs of the sensor samples at the various stages of the experiment (before wetting, wet, and after drying in air) are shown at the right. **(b)** Optical reflection spectra of the dry all-polymer film (black trace), the all-polymer film wetted with 70 % isopropyl alcohol (red trace), and the all-polymer film after the alcohol solution has dried for ~ 2 min in air (green trace). The all-polymer sensor film was prepared by thermal infiltration of a polycarbonate sheet into the pSi template and dissolution of the template as described in the text. Because this film no longer contains a pSi component, the sample displays a single stop band, which is associated with the photonic nanostructure in the polymer replica. A distinct red shift is observed for both types of photonic disks when they are infiltrated with liquid.

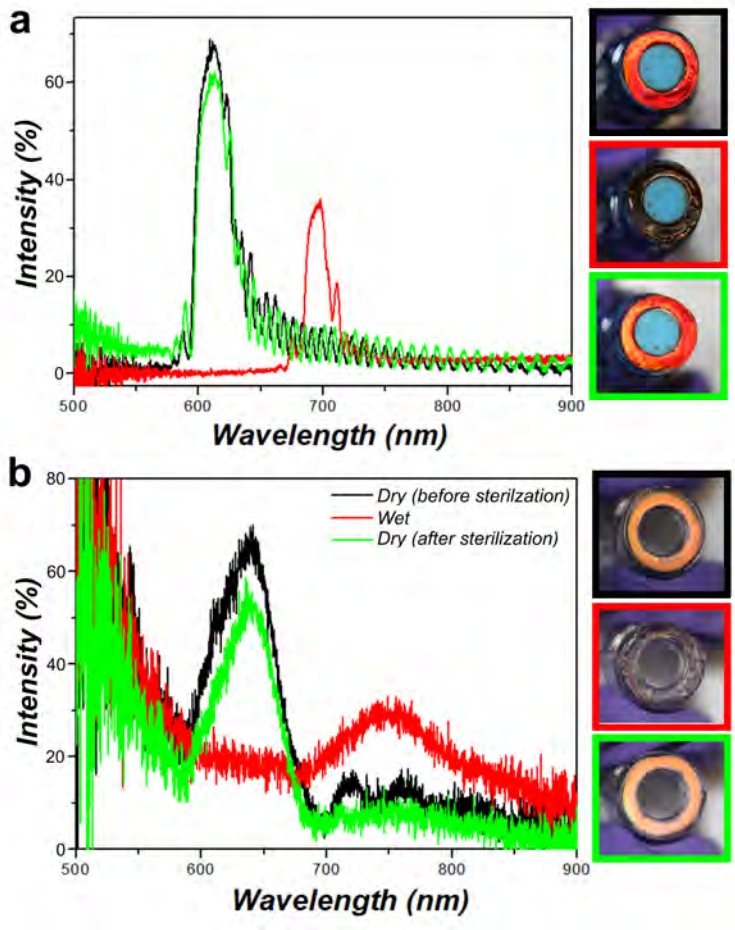

Figure S4. Optical reflection spectra of red colored pSi-polycarbonate composite (a) and all-polymer (b) samples integrated into IV connector hub units. The pSi templates in these experiments were engineered such that they appeared red when dry. Upon infiltration of ethanol, the sensor appears black as the reflection stop-band shifts to the NIR region of the spectrum, which is not visible to the human eye. Thus the these fixtures would appear to undergo a white to black transition to a color-blind individual. Optical reflection spectra and digital photographs of the pSi-polymer composite and polymer sterilization sensor embedded in IV connector hubs were obtained using the same measurement conditions as given in Figure S3, except the spectra here were corrected for instrument spectral response by ratioing to the spectrum of a silver mirror. The sinusoidal waveform used to prepare the pSi templates for these devices were etched by varying the current density between 100 to 200 mA cm^{-2} for 300 and 250 repeats for the pSi-polymer composite and the all-polymer sensors, respectively. The period of the sinusoidal waveform for the pSi-polymer composite device was 2.2 sec and for the all-polymer device it was 1.9 sec. Reflection spectra and digital photographs of samples correspond to dry (black trace or outline), wetted with 70 % isopropyl alcohol (red trace or outline), and after the alcohol solution has dried for ~ 2 min in air (green trace or outline).

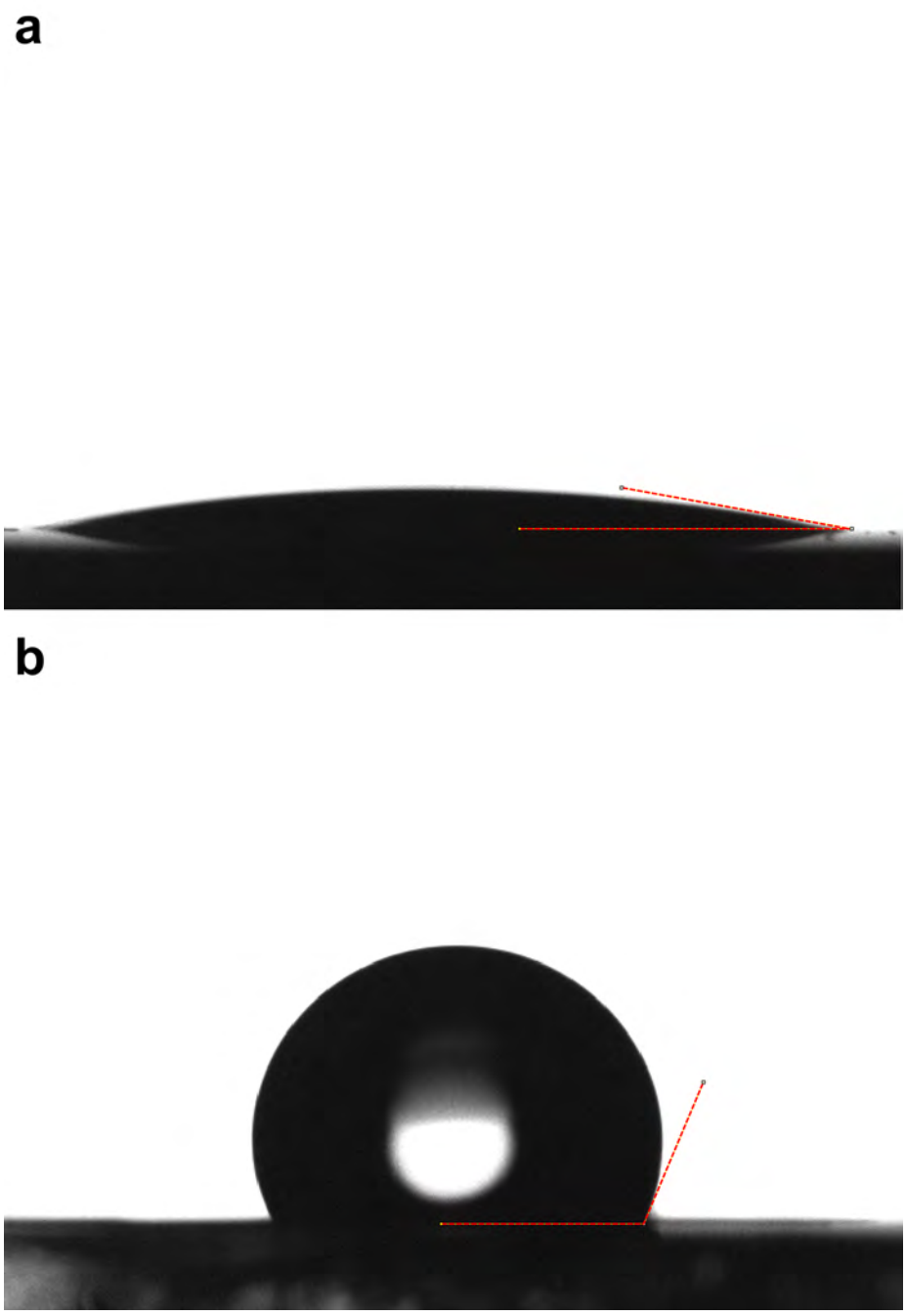

Figure S5. Water contact angle measurements of (a) an oxidized porous Si sample and (b) an all-polymer porous photonic structure. Digital photograph of a 5-10 µL droplet on the two types of sensors were obtained using a contact angle goniometer (Model No. 190-F2, Ramé-hart instrument co). The average measured contact angle was (a) 11.6° and (b) 113.8°. Error in contact angle values ± 4°.

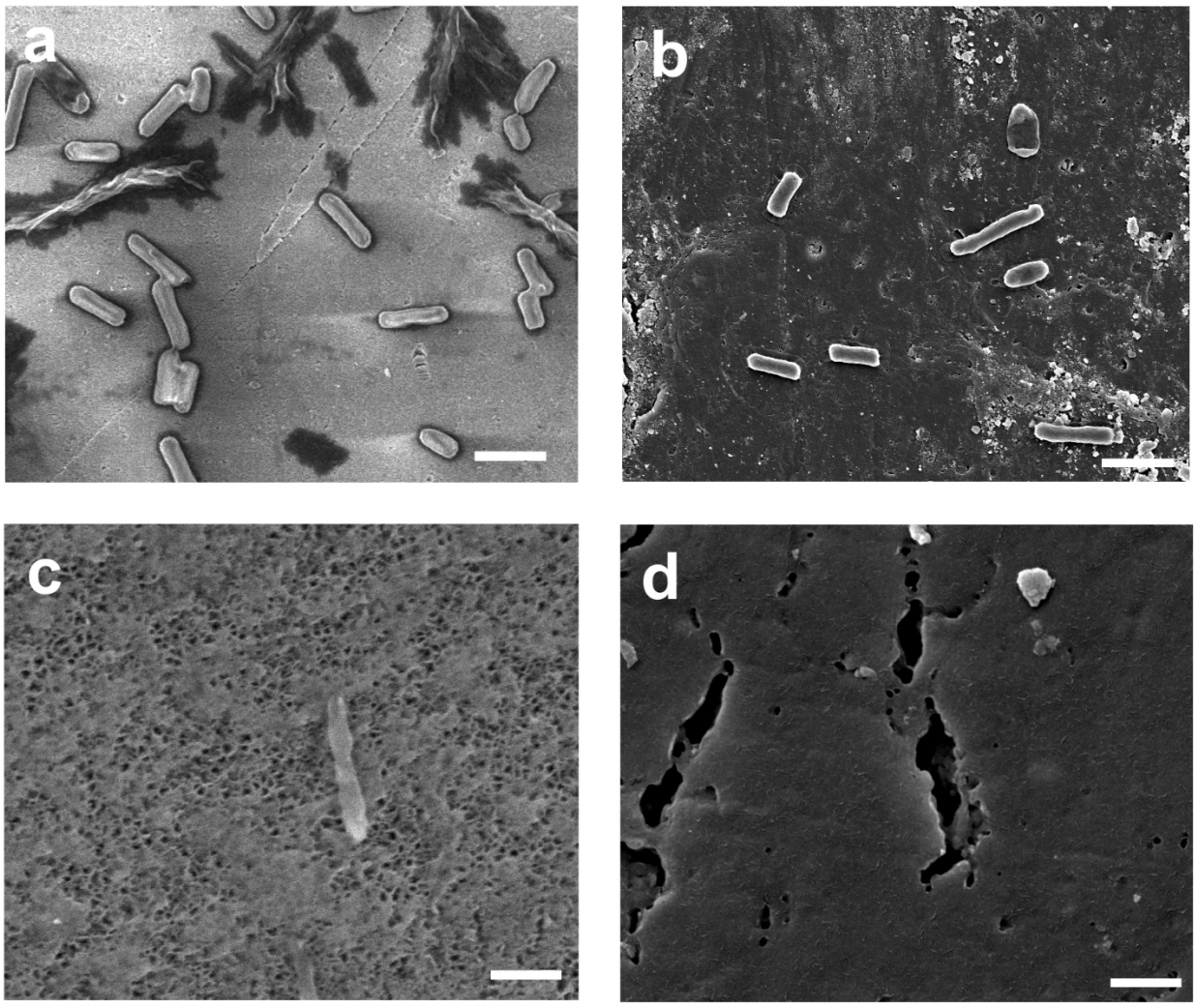

Figure S6. Electron microscope images of pSi-polymer composite (a, c) and all-polymer (b, d) IV connector hubs exposed to bacteria. Representative plan-view scanning electron microscope images of Escherichia coli adhered to the surface of the two different sensor types before (**a, b**) and after (**c, d**) sterilization with isopropyl alcohol. Sensors were incubated with 2 x 10^6 $CFU \cdot mL^{-1}$ of E. coli for images **a** and **b**. E. coli counts on both types of sensor displayed no detectable bacteria after swabbing with 70 % isopropyl alcohol-saturated tissue for 30 sec. Images **c** and **d** show some evidence of residual debris in the mesopores. Scale bar for **a** and **b**: 2 µm, Scale bar for **c** and **d**: 200 nm.

Table S1. Porosity, Thickness, and Color of Sensors

Porosity and thickness values determined using the indicated methods[a] for the templates used to prepare the pSi-polymer composite and the all-polymer photonic sensors.

Sensor Type	Thickness (μm)			Porosity (%)		λ_{sb}, pSi as-etched[b]	λ_{sb}, pSi post-ox[c]	λ_{sb}, final device[d]
	SEM	SLIM	Grav.	SLIM	Grav.			
pSi-polymer composite sensor	67.3 ± 0.3	61 ± 4	57 ± 1	60 ± 2	65 ± 2	560 nm	525 nm	550 nm
All-polymer sensor	43.0 ± 0.2	38 ± 2	42 ± 1	61 ± 1	62 ± 2	592 nm	538 nm	447 nm

[a] SEM is thickness of pSi photonic crystals before oxidation measured from cross-sectional scanning electron microscope images; SLIM refers to the Spectroscopic Liquid Infiltration Method, a non-destructive optical measurement that determines film thickness and porosity from the optical constants and the Fabry-Perot interference spectrum;[1] Grav. is a gravimetric measurement based on mass changes as described in reference ([1]).

[b] Wavelength of the maximum in the stop band reflection measured on the pSi template, as-etched but prior to oxidation or polymer infiltration.

[c] Wavelength of the maximum in the stop band reflection measured on the pSi template, after oxidation but prior to polymer infiltration. Oxidation was performed in air at 500 °C for 2 hrs.

[d] Wavelength of the maximum in the stop band reflection measured on the final sensor fixture. For the pSi-polymer device, this corresponds to the pSi template after partial thermal infiltration of polycarbonate. For the all-polymer device, this corresponds to the pSi template that had been thermally infiltrated with polycarbonate and then treated with DMSO/HF(aq) etchant to remove residual pSi from the device.

Table S2. Bacterial counts on photonic sensors before and after sterilization.

Sample	Bacteria concentration (CFU/mL)[a]	
	Bacteria Adhered[c]	***After sterilization***
pSi-polymer composite photonic IV connector hub	150000 ± 41000	N.D.
All-polymer photonic IV connector hub	71000 ± 23000	N.D.

[a] Sensors embedded in polycarbonate IV connector hubs were incubated in 2 x 10^6 CFU/mL of non-pathogenic E. coli (FDA strain Seattle 1946) in Luria-Bertani (LB) media for 4 hr. Sterilization performed on sensors by alcohol swab (70% isopropyl alcohol) following published CDC protocol.[2]

[b] N.D. = not detected. The LOD for the method was 25 CFU/mL. Error values calculated based on agar plate data from 3 samples, with serial dilutions of 1x (no dilution), 100x, 1000x, and 10,000x for each e-coli plating test.

[c] Bacteria counts reported from the agar plates inoculated with 1000x dilutions of e-coli.

Videos:

Video S1: This video shows visible changes in color upon treatment of a pSi-polymer composite photonic disk with a 70 % isopropyl alcohol-saturated swab. The color changes from green to red when swabbed with the disinfectant and returns to green after evaporation of the solution.

Video S2: This video shows visible changes in color upon treatment of an all-polymer photonic disk with a 70 % isopropyl alcohol-saturated swab. The color changes from blue to light green when swabbed with the disinfectant and returns to blue after evaporation of the solution.

Video S3: This video shows visible changes in color upon treatment of a pSi-polymer composite sensor embedded in an IV connector hub with a 70 % isopropyl alcohol-saturated swab. The color changes from green to red when swabbed with the disinfectant and returns to green after evaporation of the solution.

Video S4: This video shows visible changes in color upon treatment of an all-polymer photonic sensor embedded in an IV connector hub with a 70 % isopropyl alcohol-saturated swab. The color changes from blue to green when swabbed with the disinfectant and returns to blue after evaporation of the solution.

Video S5: This video tests for leakage around the connector hub when an infusate (PBS) is pushed through the integrated pSi-polymer composite sensor - IV connector hub assembly. No leakage was observed through repeated cycles.

References

1. Sailor, M. J., *Porous Silicon in Practice: Preparation, Characterization, and Applications*. Wiley-VCH: Weinheim, Germany, 2012; p 249.
2. O'Grady, N. P.; Alexander, M.; Burns, L. A.; Dellinger, E. P.; Garland, J.; Heard, S. O.; Lipsett, P. A.; Masur, H.; Mermel, L. A.; Pearson, M. L.; Raad, I. I.; Randolph, A. G.; Rupp, M. E.; Saint, S., Guidelines for the Prevention of Intravascular Catheter-related Infections. *Clin. Infect. Dis.* **2011,** *52* (9), e162-e193.